

# Solar Plasma Radio Emission in the Presence of Imbalanced Turbulence of Kinetic-Scale Alfvén Waves

O. Lyubchik<sup>1</sup>  · E.P. Kontar<sup>2</sup> · Y.M. Voitenko<sup>3</sup> ·  
N.H. Bian<sup>2</sup> · D.B. Melrose<sup>4</sup> 

Received: 24 February 2017 / Accepted: 10 July 2017 / Published online: 16 August 2017  
© Springer Science+Business Media B.V. 2017

**Abstract** We study the influence of kinetic-scale Alfvénic turbulence on the generation of plasma radio emission in the solar coronal regions where the ratio  $\beta$  of plasma to magnetic pressure is lower than the electron-to-ion mass ratio  $m_e/m_i$ . The present study is motivated by the phenomenon of solar type I radio storms that are associated with the strong magnetic field of active regions. The measured brightness temperature of the type I storms can be up to  $10^{10}$  K for continuum emission, and can exceed  $10^{11}$  K for type I bursts. At present, there is no generally accepted theory explaining such high brightness temperatures and some other properties of the type I storms. We propose a model with an imbalanced turbulence of kinetic-scale Alfvén waves that produce an asymmetric quasi-linear plateau on the upper half of the electron velocity distribution. The Landau damping of resonant Langmuir waves is suppressed and their amplitudes grow spontaneously above the thermal level. The estimated saturation level of Langmuir waves is high enough to generate observed type I radio emission at the fundamental plasma frequency. Harmonic emission does not appear in our model because the backward-propagating Langmuir waves undergo strong Landau damping. Our model predicts 100% polarization in the sense of the ordinary (o-) mode of type I emission.

**Keywords** Radio bursts, type I · Turbulence · Waves, Alfvén · Corona

---

Combined Radio and Space-based Solar Observations: From Techniques to New Results  
Guest Editors: Eduard Kontar and Alexander Nindos

---

✉ O. Lyubchik  
[olena@mao.kiev.ua](mailto:olena@mao.kiev.ua)

<sup>1</sup> Main Astronomical Observatory, National Academy of Sciences of Ukraine, 27 Akademika Zabolotnoho St., 03680 Kyiv, Ukraine

<sup>2</sup> School of Physics and Astronomy, University of Glasgow, G12 8QQ, Scotland, UK

<sup>3</sup> Solar-Terrestrial Centre of Excellence, Belgian Institute for Space Aeronomy, Ringlaan 3 Avenue Circulaire, 1180 Brussels, Belgium

<sup>4</sup> Sydney Institute for Astronomy, School of Physics, University of Sydney, NSW 2006, Sydney, Australia

## 1. Introduction

Numerous observations indicate that Alfvén waves are present throughout the solar atmosphere (see introduction in Morton, Tomczyk, and Pinto, 2015 and references therein). At small scales, where the perpendicular wavelength is close to the kinetic plasma scales (ion gyroradius  $\rho_i$  and/or electron inertial length  $d_e$ ), Alfvén waves transform into dispersive Alfvén waves (DAWs) with the following dispersion relation (Hasegawa and Chen, 1975; Goertz and Boswell, 1979; Lysak and Lotko, 1996; Stasiewicz *et al.*, 2000):

$$\omega = k_{A\parallel} V_A \sqrt{\frac{1 + k_{A\perp}^2 \rho_T^2}{1 + k_{A\perp}^2 d_e^2}}, \quad (1)$$

where  $\omega$  is the wave frequency and  $k_{A\parallel}$  and  $k_{A\perp}$  are wave-vector components parallel and perpendicular to the mean magnetic field  $\mathbf{B}_0$ ;  $\rho_T = \sqrt{1 + T_e/T_i} \rho_i$ ;  $\rho_i = V_{Ti}/\omega_{Bi}$  is the ion gyroradius;  $V_{Ti} = \sqrt{T_i/m_i}$  is the ion thermal velocity;  $\omega_{Bi} = q_i B_0/(m_i c)$  is the ion gyrofrequency;  $d_e = c/\omega_{pe} = c\sqrt{m_e}/\sqrt{4\pi n_0 |q_e|}$  is the electron inertial length;  $V_A = B_0/\sqrt{4\pi n_0 m_i}$  is the Alfvén velocity;  $n_0$  is the plasma number density; and  $q_s$ ,  $m_s$ , and  $T_s$  are the elementary charge, mass, and temperature of particles ( $s = i$  for the ions and  $s = e$  for the electrons). Note that in the equations  $T_s$  is expressed in energy units. We consider a hydrogen plasma where  $q_i = |q_e| = e$ , with  $e$  the proton charge. DAWs are called inertial Alfvén waves (IAWs) when the inertial term dominates in Equation 1, and they are called kinetic Alfvén waves (KAWs) when the kinetic term dominates in Equation 1.

The inertia of electrons plays a significant role in rarefied plasmas where the magnetic field is strong enough to make  $\beta < m_e/m_i \ll 1$ . On the other hand, in an intermediate  $\beta$  plasma ( $m_e/m_i \ll \beta \ll 1$ ), the effects due to a finite Larmor radius become dominant in DAWs. Recent observations have clearly demonstrated that the DAW turbulence exists in  $\beta > m_e/m_i$  plasma environments, such as the solar wind (He *et al.*, 2012), and also in  $\beta < m_e/m_i$  plasma environments, such as the auroral zones below 4 Earth radii (Chaston *et al.*, 2008). DAWs cannot be observed directly in the solar corona. However, spectral line observations indicate that there are many unresolved nonthermal motions that imply Alfvén waves with velocity amplitudes of  $\approx 30 \text{ km s}^{-1}$  and higher (Banerjee *et al.*, 1998).

The parallel electric field of DAWs makes them efficient in Cherenkov resonant interaction with plasma particles. The ion and electron dynamics in the solar wind under the influence of KAW turbulence was examined by Rudakov *et al.* (2012). It was shown that the particle diffusion governed by KAWs leads to the development of a plateau in the electron distribution and to a step-like distribution for the superthermal ions. These distributions are found to be unstable to electromagnetic waves due to ion cyclotron resonance. The analytic theory of proton diffusion driven by the KAW spectra observed in the solar wind was developed by Voitenko and Pierrard (2013). These authors performed kinetic simulations of the velocity-space diffusion of protons (Pierrard and Voitenko, 2013). It was shown that the presence of Alfvénic turbulence in the solar wind leads to a fast development of nonthermal tails in the proton velocity distribution function. The tails are already noticeable at distances of about one solar radius from the simulation boundary, and they increase rapidly with radial distance and become pronounced beyond 2–3 solar radii.

Note that DAWs can resonantly exchange energy with particles in the velocity range between the Alfvén velocity  $V_A$  and the electron thermal velocity  $V_{Te}$ . In the solar atmosphere, usually  $V_A < V_{Te}$ , and DAWs are usually not efficient agents for resonant acceleration of coronal electrons to suprathermal energies (see, however, Artemyev, Zimovets, and Rankin, 2016). Favorable conditions for the suprathermal electron acceleration are found in regions

with strong magnetic fields and/or low temperatures, where the electron thermal speed drops below the Alfvén speed,  $V_A > V_{Te}$ . In such regions, DAW turbulence leads to the diffusive acceleration of resonant suprathermal electrons to Alfvénic velocities, creating a quasi-linear plateau on the electron velocity distribution.

The purpose of this article is to study possible effects of the IAW turbulence in the generation of solar coronal radio emission. The proposed scenario is as follows. First, the IAW turbulence produces a flat (plateau-like) velocity distribution of the electrons in the velocity range  $\sqrt{1 + T_i/T_e} V_{Te} < V_{\parallel} < V_A$ . This local flattening of the velocity distribution suppresses the Landau damping of the resonant Langmuir waves (LWs), which in turn enables their spontaneous growth to high nonthermal levels. Then the resulting high-amplitude LWs can interact nonlinearly with low-frequency plasma waves, generating electromagnetic radiation (radio waves) close to the local plasma frequency.

Our scenario can contribute to radio emission from the coronal regions where the ratio  $\beta$  of plasma to magnetic pressure is lower than the electron-to-ion mass ratio  $m_e/m_i$ . In particular, this mechanism can account for type I solar radio storms – the most common manifestations of solar radio emission at meter wavelengths (Elgarøy, 1977; McLean and Labrum, 1985).

The outline of the article is as follows. The influence of the IAW turbulence on the electron velocity distribution and the spectral energy density of Langmuir waves are estimated in Section 2. The theory for fundamental plasma emission by the fusion/decay processes  $L \pm S \rightarrow T$  is presented in Section 3, including the rate equations for the emission processes (Section 3.1), the saturation level of fundamental plasma emission (Section 3.2), and its absorption during propagation (Section 3.3). Possible application to type I solar radio bursts is discussed in Section 4. Our main conclusions are given in Section 5.

## 2. Spectral Energy Density of LWs due to IAW Turbulence

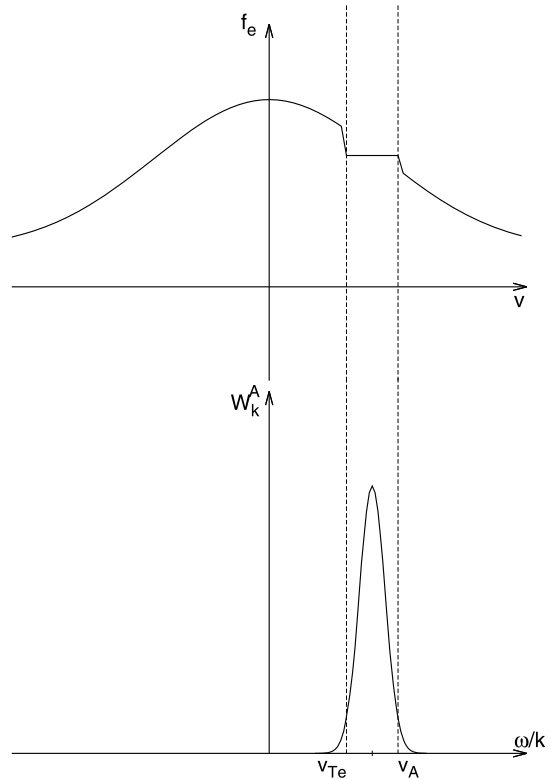
The Landau resonance with electrons is made possible by the existence of a parallel electric field that is the result of the combined effect of the electron pressure gradient and electron inertia in Ohm's law. This parallel electric field is also the very reason for the wave dispersion (see Equation 1) in a collisionless plasma. In the case  $\rho_T = d_e$ , the wave becomes dispersionless and the wave-particle resonance reduces to a single point in velocity-space (see Appendix A for the details). Otherwise, the range of Landau resonance in velocity-space is finite. The generation of a spectrum of parallel electric field fluctuations by Alfvénic turbulence was studied in Bian, Kontar, and Brown (2010). Parallel electric field amplification and spectral formation by phase mixing of Alfvén waves were studied in Bian and Kontar (2011), and the role of this electric field in the bulk energization of electrons during solar flares was developed in Melrose and Wheatland (2014).

The Landau resonance between electrons and DAWs occurs when the electron velocity  $V_{\parallel}$  is equal to the wave phase speed  $V_{DAW} = \omega/k_{A\parallel}$ , *i.e.*

$$V_{\parallel} = V_A \sqrt{\frac{1 + k_{A\perp}^2 \rho_T^2}{1 + k_{A\perp}^2 d_e^2}}.$$

The range of resonant velocities extends from  $V_{\parallel} = V_T = \sqrt{1 + T_i/T_e} V_{Te}$  at  $k_{A\perp} \rightarrow \infty$  to  $V_{\parallel} = V_A$  at  $k_{A\perp} \rightarrow 0$ . Note that we are interested in the regions where the plasma  $\beta$  can be smaller than the electron-to-ion mass ratio  $m_e/m_i$ . In this low- $\beta$  plasma the DAWs are IAWs, and phase velocities are higher than the electron thermal velocity  $V_{Te}$ .

**Figure 1** Time-asymptotic electron velocity distribution  $f_e$  modified by the IAW spectrum  $W_k^A$ . The quasi-linear diffusion establishes a plateau on the initially Maxwellian distribution in the resonant velocity range  $\sqrt{1 + T_i/T_e} V_{Te} < V_{\parallel} < V_A$ . Outside this interval, the velocity distribution remains Maxwellian.



Starting from the initially Maxwellian velocity distribution, the quasi-linear plateau can be formed by IAWs in the resonant velocity range  $\sqrt{1 + T_i/T_e} V_{Te} < |V_{\parallel} = V_{IAW}| < V_A$ , as is sketched in Figure 1. This process is essentially the same as the quasi-linear evolution of initially Maxwellian velocity distributions driven by KAWs in the solar wind, which has been studied by Rudakov *et al.* (2012), Voitenko and Pierrard (2013), and Pierrard and Voitenko (2013). The particle beams are not needed for this. In turn, the reduced velocity-space gradient within the plateau suppresses the linear Landau damping of resonant LWs with phase velocities  $\sqrt{1 + T_i/T_e} V_{Te} < V_{LW} < V_A$ . As a consequence, a spontaneous growth of LW amplitudes is possible in this velocity range.

We have to note that the initial velocity distribution of the electrons does not have to be exactly Maxwellian, it can be *e.g.* a kappa-distribution, as is often observed in space. However, this would not affect the IAW dispersion and polarization, which depend on the bulk plasma parameters, and the basic physical picture would be the same. First, the IAWs flatten the electron velocity distribution in the resonant velocity range, which is then followed by the spontaneous growth of the Langmuir wave amplitudes above the thermal level.

In situ satellite observations have revealed that the magnetohydrodynamic (MHD) Alfvénic turbulence in the solar wind is dominated by the anti-sunward wave flux (Bruno and Carbone, 2013, and references therein). The corresponding wave turbulence is referred to as imbalanced. Matthaeus *et al.* (1999) suggested that the imbalanced turbulence of MHD Alfvén waves also develops in the solar corona, where it can reach dissipative scales and heat the plasma. Voitenko and De Keyser (2016) investigated the MHD-kinetic turbulence transition and showed that the KAW turbulence is less imbalanced than the parent MHD

turbulence, but remains imbalanced throughout. Other possible sources for the imbalanced KAW turbulence in the solar corona include phase mixing (Voitenko and Goossens, 2000) and magnetic reconnection (Voitenko, 1998). In solar flares these KAWs can lead to impulsive plasma heating (Voitenko, 1998) and non-local electron acceleration to relativistic energies (Artemyev, Zimovets, and Rankin, 2016).

In contrast to the balanced IAW turbulence, which is symmetric with respect to  $k_{\parallel} \rightarrow -k_{\parallel}$ , the wave amplitudes in the imbalanced IAW turbulence are much smaller at  $k_{\parallel} < 0$  than at  $k_{\parallel} > 0$ . The balanced IAW turbulence forms two symmetric quasi-linear plateaus in the electron velocity distribution function (VDF), at  $-V_A < V_{\parallel} < -\sqrt{1 + T_i/T_e} V_{Te}$  and  $\sqrt{1 + T_i/T_e} V_{Te} < V_{\parallel} < V_A$ . The imbalanced IAW turbulence forms the plateaus asymmetrically, preferentially in the propagation direction of the dominant IAW component, which we take as positive, *i.e.* at  $\sqrt{1 + T_i/T_e} V_{Te} < V_{\parallel} < V_A$ . The spontaneous emission of LWs can be studied independently for forward and backward plateaus.

As the origin of coronal Alfvén waves is at the coronal base, it is natural to expect that the upward wave flux in the solar corona is higher than the downward flux and that the corresponding turbulence is imbalanced. The turbulence imbalance has a striking consequence in our scenario. As the quasi-linear plateau is formed by the IAW turbulence preferentially in the direction of the dominant upward-propagating IAW fraction, *i.e.* at  $\sqrt{1 + T_i/T_e} V_{Te} < V_{\parallel} < V_A$ , the Landau damping of upward-propagating Langmuir waves is highly reduced in this velocity range and they can grow spontaneously to high amplitudes. In contrast, the downward IAW flux is weaker and not as efficient in forming the plateau, in which case the Landau damping of downward Langmuir waves remains strong and prevents their spontaneous growth. In these conditions, there are no counter-propagating Langmuir waves, and only fundamental radio emission can be generated by the plasma emission mechanism.

In the 1D approximation, the governing equation for the spectral energy density of LWs is (Vedenov and Velikhov, 1963; Ryutov, 1969; Hamilton and Petrosian, 1987)

$$\frac{dW_k^l}{dt} = \frac{\pi \omega_{pe}^3}{n_e k^2} W_k \left[ \frac{\partial f}{\partial V} \right]_{V=\omega_{pe}/k} + \frac{\omega_{pe}^3 m_e}{4\pi n_e} \left[ V \ln \left( \frac{V}{V_{Te}} \right) f \right]_{V=\omega_{pe}/k} - \gamma_{coll} W_k^l, \quad (2)$$

where  $W^l(k, t)$  [ergs cm<sup>-2</sup>] is the spectral energy density of LWs,  $f(V, t)$  [electrons cm<sup>-3</sup> (cm/s)<sup>-1</sup>] is the electron distribution function,  $k$  is the LW wavenumber (we are mostly interested in parallel-propagating LWs with  $k \equiv k_{\parallel}$ ),  $V$  is the parallel component of the particle velocity ( $V \equiv V_{\parallel}$ ), and  $\omega_{pe}$  is the local electron plasma frequency. Here the following normalizations are used:

$$\int_{-\infty}^{\infty} f dV = n_e,$$

where  $n_e$  is the density of the background plasma in cm<sup>-3</sup> and

$$\int_{-k_{De}}^{k_{De}} W_k^l dk = W^l,$$

where  $W^l$  is the total energy density of the waves in ergs cm<sup>-3</sup>, with  $k_{De} = \omega_{pe}/V_{Te}$ . The first term on the right-hand side (RHS) of Equation 2 describes the induced absorption of plasma waves by electrons (Landau damping), and the second term describes the spontaneous emission. This emission (and the corresponding absorption) is resonant, meaning an electron at velocity  $V$  interacts only with a wave at wavenumber  $k = \omega_{pe}/V$ . Collisional

damping of LWs is given by the third term on the RHS, where  $\gamma_{\text{coll}} = \frac{1}{3} \sqrt{\frac{2}{\pi}} \frac{\Gamma}{V_{\text{Te}}^3} \simeq \Gamma / (4V_{\text{Te}}^3)$  with  $\Gamma = 4\pi e^4 n_e \ln \Lambda / m_e^2$ , where  $\ln \Lambda$  is the Coulomb logarithm (approximately 20 in the solar corona).

According to Equation 2, the spectral energy density of LWs in the resonant range is

$$W_k^l = \frac{1}{\gamma_{\text{coll}}} \frac{\omega_{\text{pe}}^3 m_e}{4\pi n_e} \left[ V \ln \left( \frac{V}{V_{\text{Te}}} \right) f \right]_{V=\omega_{\text{pe}}/k} \tag{3}$$

The local plateau function  $f_{\text{pl}}$  can be found from conservation of resonant particles:  $\int_{V_{\text{min}}}^{V_{\text{max}}} [f(V, \infty) - f(V, 0)] dV = 0$ , and  $f(V, \infty) = \text{const}$ . Following Voitenko and Pierrard (2013), we express  $f_{\text{pl}}$  in terms of an error function:

$$\begin{aligned} f_{\text{pl}} &= \frac{1}{\Delta V} \int_{V_{\text{min}}}^{V_{\text{max}}} f_M dV \\ &= \frac{n_e}{\Delta V} \frac{\text{erf}(V_{\text{max}}/\sqrt{2}V_{\text{Te}}) - \text{erf}(V_{\text{min}}/\sqrt{2}V_{\text{Te}})}{2}, \end{aligned} \tag{4}$$

where  $\Delta V = V_{\text{max}} - V_{\text{min}}$ ,  $V_{\text{max}}$  ( $V_{\text{min}}$ ) is the maximum (minimum) velocity of the electrons involved in the plateau, and  $f_M$  is the Maxwellian distribution. Since in the solar corona  $\beta$  cannot be much smaller than  $m_e/m_i$ , the IAWs resonate within a narrow range of phase velocities, and quasi-linear diffusion should be fast enough to create the plateau from  $V_{\text{min}} \approx \sqrt{1 + T_i/T_e} V_{\text{Te}}$  to  $V_{\text{max}} \approx V_A$ .

Consequently, the normalized spectral energy of LWs takes the following form:

$$\frac{W_k^l}{W_{\text{th}}^l} = \pi \frac{V_{\text{Te}}}{\Delta V} \frac{\omega_{\text{pe}}}{\gamma_{\text{coll}}} \frac{1}{k^3 \lambda_{\text{De}}^3} \frac{\text{erf}(V_A/\sqrt{2}V_{\text{Te}}) - \text{erf}(\sqrt{1 + T_i/T_e}/\sqrt{2})}{2}, \tag{5}$$

where the thermal level of LWs is given by (Kontar, Ratcliffe, and Bian, 2012; Ratcliffe and Kontar, 2014):

$$\begin{aligned} W_{\text{th}}^l &= \frac{T_e}{4\pi^2} \frac{k^2 \ln\left(\frac{1}{k\lambda_{\text{De}}}\right)}{1 + \frac{\gamma_{\text{coll}}}{\omega_{\text{pe}}} \sqrt{\frac{2}{\pi}} k^3 \lambda_{\text{De}}^3 \exp\left[\frac{1}{2k^2 \lambda_{\text{De}}^2}\right]} \\ &\simeq \frac{T_e}{4\pi^2} k^2 \ln\left(\frac{1}{k\lambda_{\text{De}}}\right). \end{aligned} \tag{6}$$

Figure 2 shows the normalized spectral energy density of Langmuir waves in the resonant wavenumber range  $V_{\text{Te}}/V_A < k\lambda_{\text{De}} < 0.82$ . We have considered two types of possible coronal plasma parameters for the heliocentric distances  $R/R_{\odot} \approx 1.1$  with  $n_0 = 2.8 \times 10^8 \text{ cm}^{-3}$  or  $f_{\text{pe}} = 150 \text{ MHz}$  (Warmuth and Mann, 2005). The first has  $T_e = 10^6 \text{ K}$  and a stronger magnetic field in the range  $B_0 = 150\text{--}40 \text{ G}$  (Figure 2a). The second has a lower temperature  $T_e = 10^5 \text{ K}$  and a weaker magnetic field in the range  $B_0 = 50\text{--}13 \text{ G}$  (Figure 2b). Values like this for  $B_0$  from 10 to 150 G and  $T_e$  from  $10^5 \text{ K}$  to  $10^6 \text{ K}$  (the temperature could be even lower, down to  $10^4 \text{ K}$ ) are supported by recent observations (see articles by Schad *et al.*, 2016; Antolin *et al.*, 2015) for the relevant heliocentric distances  $R/R_{\odot} \approx 1.1$ . As is seen from Figure 2, the normalized spectral energy density of LWs reaches its maximum value

$$W_k^l / W_{\text{th}}^l \simeq 6 \times 10^8, \tag{7}$$

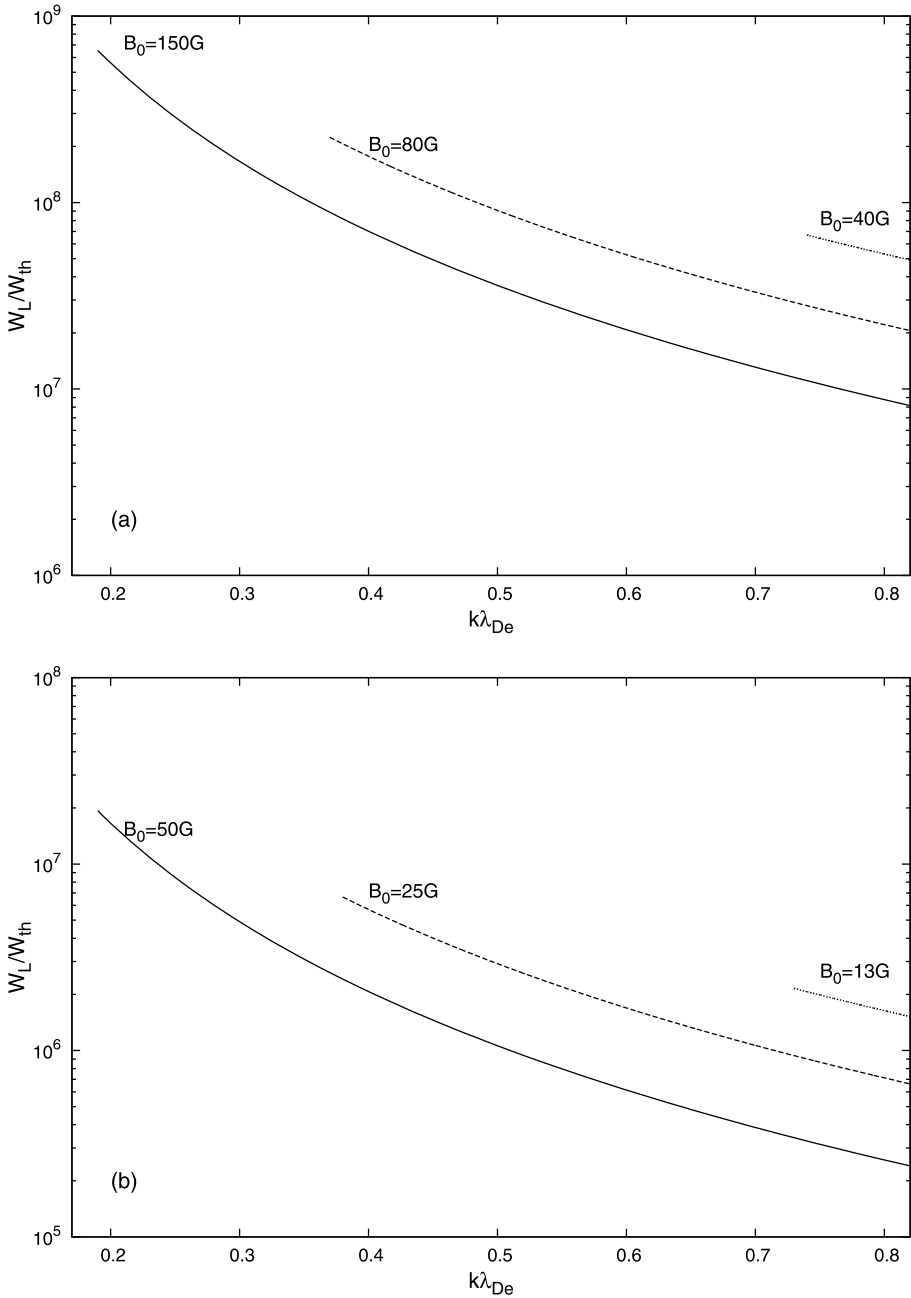


**Figure 2** Normalized spectral energy density of Langmuir waves in the resonant wavenumber range  $V_{Te}/V_A < k\lambda_{De} < 0.82$ . The plasma parameters are  $n_0 = 2.8 \times 10^8 \text{ cm}^{-3}$ ;  $T_i/T_e = 0.5$ . Case (a) corresponds to  $T_e = 10^6$  K and three values of magnetic field strength  $B_0 = 150, 80$  and  $40$  G. Case (b) corresponds to  $T_e = 10^5$  K and three values of magnetic field strength  $B_0 = 50, 25$  and  $13$  G.

for  $B_0 = 150$  G,  $T_e = 10^6$  K and

$$W_k^l / W_{th}^l \simeq 2 \times 10^7, \tag{8}$$

for  $B_0 = 50$  G,  $T_e = 10^5$  K and for the resonant velocities of LWs close to the upper boundary,  $V_{LW} \lesssim V_A$ , which corresponds to LW wavenumbers  $k\lambda_{De} \gtrsim 0.19$ . For lower values of the magnetic field strength, the normalized spectral energy density of LWs is still high, whereas the resonance wavenumber range becomes narrower.

This high level of LWs is obtained under the conditions that the quasi-linear Landau damping of LWs (first term in the RHS of Equation 2) is weaker than their collisional damping (third term). When the slope of the plateau is large enough to make the Landau damping dominant, the spontaneous growth of LWs is reduced. Using results by Voitenko and Goossens (2006), we estimated that this first term is smaller than the third for realistic IAW parameters, and consequently, the state of saturation is governed by the balance between the second and third terms.

### 3. Fundamental Plasma Emission from the IAW Turbulent Plasma

#### 3.1. Kinetic Equations for the Spectral Energy Density of Transverse Waves due to the Process $L \pm S \rightarrow T$

We consider the theory of fundamental plasma emission generated by the nonlinear fusion  $L + S \rightarrow T$  (hereafter  $f$ -process), and/or decay  $L \rightarrow T + S$  (hereafter  $d$ -process). Here  $L$  is the Langmuir wave,  $S$  is the ion sound wave (ISW), and  $T$  is the transverse radio wave. The kinetic equations for fundamental emission by the processes  $L \pm S \rightarrow T$  are based on the general expressions in Melrose (1980b) and Tsytovich and ter Haar (1995),

$$\begin{aligned} \frac{dW_{T\pm}(k_T)}{dt} &= \frac{\omega_T}{\hbar} \int \frac{dk_L dk_S}{(2\pi)^3} u_{TLS\pm}(k_T, k_L, k_S) \\ &\times \left[ \frac{W_L}{\omega_L} \left( \frac{W_S}{\omega_S} \mp \frac{W_T}{\omega_T} \right) - \frac{W_T}{\omega_T} \frac{W_S}{\omega_S} \right], \end{aligned} \tag{9}$$

with the following emission probability

$$u_{TLS\pm} = C \frac{[k_T \times k_L]^2}{k_T^2 k_L^2} \delta(k_T - k_L \mp k_S) \delta(\omega_T - \omega_L \mp \omega_S),$$

where

$$C = \frac{\hbar e^2 (2\pi)^6}{8\pi m_e^2 V_{Te}^4} \frac{\omega_{pe}^3 \omega_S^3}{\omega_{pi}^2 k_S^2 \omega_T},$$

and the “ $\pm$ ” signs refer to the  $f$ - and  $d$ -processes, respectively. The delta functions lead to kinematic constraints on the frequencies and wave vectors of waves taking part in the considered processes. According to the energy and momentum conservation conditions,

$$\begin{aligned} \omega_L(k_L) \pm \omega_S(k_S) &= \omega_T(k_T), \\ k_L \pm k_S &= k_T, \end{aligned}$$



the wavenumbers of interacting waves must satisfy  $k_S \simeq \mp k_L$ , and the electromagnetic emission is generated approximately perpendicular to the initial LW with the wavenumber

$$k_T d_e \approx \sqrt{3} k_L \lambda_{De}. \tag{10}$$

Using an angle-averaged emission model (Ratcliffe and Kontar, 2014; Ratcliffe, 2013) that we describe in detail in Appendix B, we obtain the following equation for the spectral energy density of transverse waves:

$$\begin{aligned} \frac{dW_{T\pm}^{Av}(k_T)}{dt} &= \frac{\pi \omega_{pe}^4 V_s}{24 n_e T_e V_{Te}^2} \left(1 + \frac{3T_i}{T_e}\right) \sqrt{1 + k_T^2 d_e^2} \\ &\times \left[ \frac{W_L^{Av}(k_L)}{\omega_L} \frac{4\pi k_T^2}{\Delta\Omega k_S^2} \frac{W_S^{Av}(k_S)}{\omega_S} \mp \frac{W_L^{Av}(k_L)}{\omega_L} \frac{W_T^{Av}(k_T)}{\omega_T} - \frac{W_T^{Av}(k_T)}{\omega_T} \frac{W_S^{Av}(k_S)}{\omega_S} \right]. \end{aligned} \tag{11}$$

Rewriting this in terms of the brightness temperature,

$$k_B T_k^T = \frac{2\pi^2 W_{Tk}}{k_T^2}, \tag{12}$$

we obtain the following basic equation for the transverse wave brightness temperature induced by  $L \pm S \rightarrow T$  processes:

$$\begin{aligned} \frac{dT_{T\pm}(k_T)}{dt} &= \frac{\pi \omega_{pe}^4 V_s}{24 n_e T_e V_{Te}^2} \left(1 + \frac{3T_i}{T_e}\right) \sqrt{1 + k_T^2 d_e^2} \\ &\times \left[ \frac{\eta}{k_S^2} \frac{W_L^{Av}(k_L)}{\omega_L} \frac{W_S^{Av}(k_S)}{\omega_S} \mp \frac{W_L^{Av}(k_L)}{\omega_L} \frac{T_T(k_T)}{\omega_T} - \frac{T_T(k_T)}{\omega_T} \frac{W_S^{Av}(k_S)}{\omega_S} \right], \end{aligned} \tag{13}$$

where

$$\eta = \frac{(2\pi)^3}{\Delta\Omega},$$

and

$$k_S^2 = k_T^2 + k_L^2; k_L \approx \mp \frac{k_T d_e}{\sqrt{3} \lambda_{De}}.$$

### 3.2. Saturation Level of Plasma Emission in the Presence of Nonthermal Levels of Langmuir and Ion-Sound Waves

The condition  $dT_{T\pm}(k_T)/dt = 0$  in expression 13 defines the saturation of the  $f$ - and  $d$ -processes. Therefore, the saturation brightness is

$$T_{T+} = \omega_T \frac{\frac{\eta}{k_S^2} \frac{W_L}{\omega_L} \frac{W_S}{\omega_S}}{\frac{W_S}{\omega_S} + \frac{W_L}{\omega_L}} \tag{14}$$

for the  $f$ -process and

$$T_{T-} = \omega_T \frac{\frac{\eta}{k_S^2} \frac{W_L}{\omega_L} \frac{W_S}{\omega_S}}{\frac{W_S}{\omega_S} - \frac{W_L}{\omega_L}} \tag{15}$$

for the  $d$ -process.

We now separately discuss two cases, i)  $W_S/\omega_S \ll W_L/\omega_L$ , and ii)  $W_S/\omega_S \gg W_L/\omega_L$ .

### 3.2.1. Case i: $W_S/\omega_S \ll W_L/\omega_L$

First we consider the saturation level of the processes for the nonthermal level of LWs that is due to the spontaneous emission Equation 5 and the thermal level of ion-sound waves, which is defined by

$$W_{\text{StH}} = T_e k_{\text{De}}^2 \frac{k_{\text{De}}^2}{k_{\text{De}}^2 + k^2}. \tag{16}$$

As in this case  $W_L \gg W_S$ , then according to Equation 14  $T_{T+}$  saturates at about  $W_{\text{StH}}$  for the  $f$ -process:

$$T_{T+} = \omega_T \frac{\eta}{k_S^2} \frac{W_{\text{StH}}}{\omega_S}. \tag{17}$$

The saturation level  $T_{T-}$  for the  $d$ -process  $L \rightarrow T + S$  is defined by Equation 15. Consequently, for  $W_L \gg W_S$ , we should get exponential growth that causes both  $T_T$  and  $W_S$  to increase until  $W_S \gg W_L$ , when the process saturates at the level

$$T_{T-} = \omega_T \frac{\eta}{k_S^2} \frac{W_L}{\omega_L}, \tag{18}$$

with  $W_L$  defined by Equation 5.

Figures 3–4 show the brightness temperature  $T_T(k)$  of the fundamental radio emission for the  $f$ -process (top panel) and for the  $d$ -process (bottom panel) for two sets of parameters:  $T_e = 10^6$  K and  $B_0 = 150\text{--}40$  G, and  $T_e = 10^5$  K and  $B_0 = 50\text{--}13$  G. For both cases the values of the brightness temperature  $T_T(k)$  are rather high even for the thermal level of ion-sound waves.

### 3.2.2. Case ii: $W_S/\omega_S \gg W_L/\omega_L$

In this case, the  $f$ - and  $d$ -processes are essentially equivalent and saturate at

$$T_{T+} = T_{T-} = \omega_T \frac{\eta}{k_S^2} \frac{W_L}{\omega_L}. \tag{19}$$

It follows from Figures 3–4 (bottom panel) that the brightness temperature of radio emission is in the range  $T_{T\pm} \approx 2 \times 10^{12}\text{--}10^{15}$  K for  $T_e = 10^6$  K and  $T_{T\pm} \approx 5 \times 10^9\text{--}2 \times 10^{13}$  K for  $T_e = 10^5$  K.

We specify the nonthermal level of ion-sound waves, which is required for this to be the case. The 1D spectral energy density of ISWs is related to the spectral density of electron density fluctuation as (see Appendix C for details)

$$\frac{W_S(k)}{n_e T_e} = (1 + k_S^2 \lambda_{\text{De}}^2) \frac{|\delta n_e|_k^2}{n_e^2}. \tag{20}$$

According to the above expression, the density spectrum of the thermal level of ion sound waves corresponds to

$$\frac{|\delta n_e|_{\text{thk}}^2}{n_e^2} = \frac{4\pi}{n_e \lambda_{\text{De}}^2} \frac{k_S^2 \lambda_{\text{De}}^2}{1 + k_S^2 \lambda_{\text{De}}^2}. \tag{21}$$

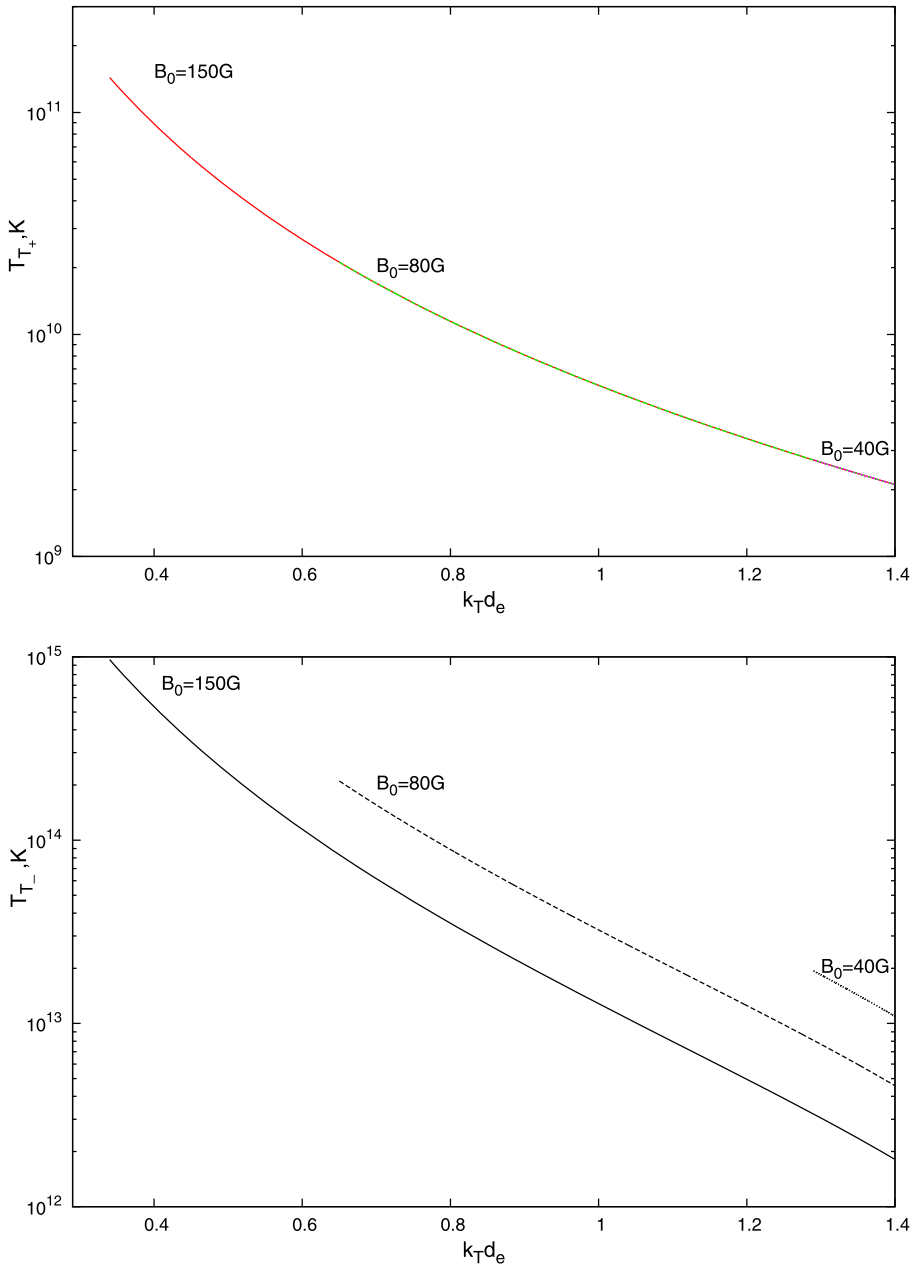


**Figure 3** Brightness temperature  $T_T(k)$  of fundamental radio emission for the  $f$ -process (top panel) and  $d$ -process (bottom panel). Here we consider a nonthermal level of LWs, thermal ISWs, and  $\eta = 4\pi^2$ . The plasma parameters are  $n_0 = 2.8 \times 10^8 \text{ cm}^{-3}$ ,  $T_e = 10^6 \text{ K}$ ,  $T_i/T_e = 0.5$ , and the three values of the magnetic field strength are  $B_0 = 150, 80, \text{ and } 40 \text{ G}$ .

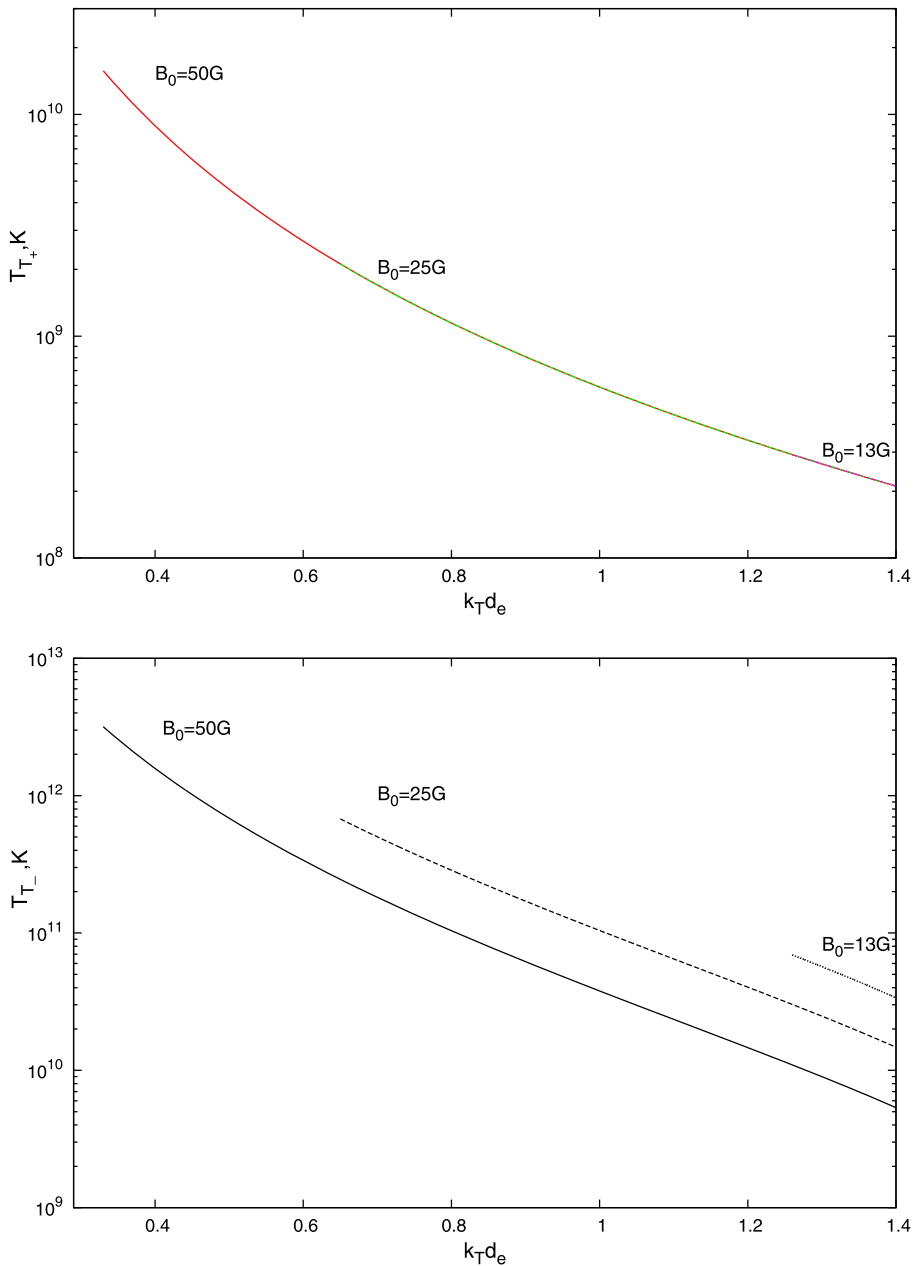


**Figure 4** Brightness temperature  $T_T(k)$  of the fundamental radio emission for the  $f$ -process (*top panel*) and the  $d$ -process (*bottom panel*). Here we consider a nonthermal level of LWs, thermal ISWs, and  $\eta = 4\pi^2$ . The plasma parameters are  $n_0 = 2.8 \times 10^8 \text{ cm}^{-3}$ ,  $T_e = 10^5 \text{ K}$ , and  $T_i/T_e = 0.5$ , and the three values of the magnetic field strength are  $B_0 = 50, 25$ , and  $13 \text{ G}$ .

In Figure 5 we present the spectral density of the electron density fluctuation for the thermal level of ion-sound waves (dotted line) and when  $W_S/\omega_S = W_L/\omega_L$  (solid, dashed, and dash-dotted lines). Consequently, for  $T_e = 10^6$  K, the case  $W_S/\omega_S \gg W_L/\omega_L$  requires a level of the ISW that is several orders of magnitude higher than the thermal level ( $|\delta n_e|_k^2/|\delta n_e|_{\text{th}k}^2 \gtrsim 10^4$  for  $k\lambda_{\text{De}} \gtrsim 0.2$ ). For the lower temperature  $T_e = 10^5$  K in the short-wavelength domain, the amplitudes of the ISWs approach the thermal level, but still remain higher than the thermal level.

Our model describes emission from active regions in the corona, where the relative level of density fluctuations is unknown. Chen *et al.* (2012) reported a measurement of the spectral index of density fluctuations between ion and electron scales in solar wind turbulence. In Figure 6 (top panel) the power spectra of the electron density fluctuations in the solar wind are shown according to Figure 2 of Chen *et al.* (2012).

Assuming that the frequency spectra are Doppler-shifted  $k$ -spectra,

$$P(k) = \frac{P(f)V}{2\pi},$$

with  $k = 2\pi f/V$  and  $V \equiv V_{\text{SW}} = 3.2 \times 10^7 \text{ cm s}^{-1}$ , we can derive the  $k$ -power spectra of solar wind electron fluctuations, see Figure 6 (bottom panel).

We extrapolated the  $k$ -power spectra of solar wind electron fluctuations (see Figure 7) into the short-wavelength domain using  $k^{-2.7}$  (dotted line) and present the spectral density of the electron density fluctuation for the thermal level of solar wind ion-sound waves (dashed line).

In the relevant range  $0.19 < k\lambda_{\text{De}} < 0.82$ , the observed density fluctuation is on the order of the thermal fluctuations. We would like to note that the observed  $-2.7$  spectra are attributed to the KAW turbulence (Chen *et al.*, 2012) rather than to ISWs, but we consider this extrapolations as the upper bound. Helios spacecraft observations at 0.3 AU (Marsch and Tu, 1990) and numerical models (Reid and Kontar, 2010) also suggest that the relative level of density fluctuations decreases toward the Sun. Consequently, it seems unlikely that the case  $W_S/\omega_S \gg W_L/\omega_L$  is realistic.

### 3.3. Absorption of Emission During the Propagation

Furthermore, we have considered the collisional absorption of radiation during propagation. According to Ratcliffe and Kontar (2014), collisional absorption (inverse bremsstrahlung) with the damping rate  $\gamma_d$  gives an optical depth

$$\tau = \int_0^{1 \text{ AU}} \frac{\gamma_d(x)}{V_g^T(x)} dx, \tag{22}$$

where

$$\gamma_d = \gamma_c \frac{\omega_{\text{pe}}^2}{\omega^2} = \frac{1}{3} \sqrt{\frac{2}{\pi}} \frac{\Gamma}{V_{\text{Te}}^3} \frac{\omega_{\text{pe}}^2}{\omega^2} = \frac{1}{3} \sqrt{\frac{2}{\pi}} \frac{e^2 \ln \Lambda}{m_e V_{\text{Te}}^3} \frac{\omega_{\text{pe}}^4}{\omega^2}, \tag{23}$$

and

$$V_g^T = \frac{\partial(\omega_{\text{pe}}^2 + k_T^2 c^2)}{\partial k_T} = \frac{c}{\omega} (\omega^2 - \omega_{\text{pe}}^2)^{1/2}. \tag{24}$$

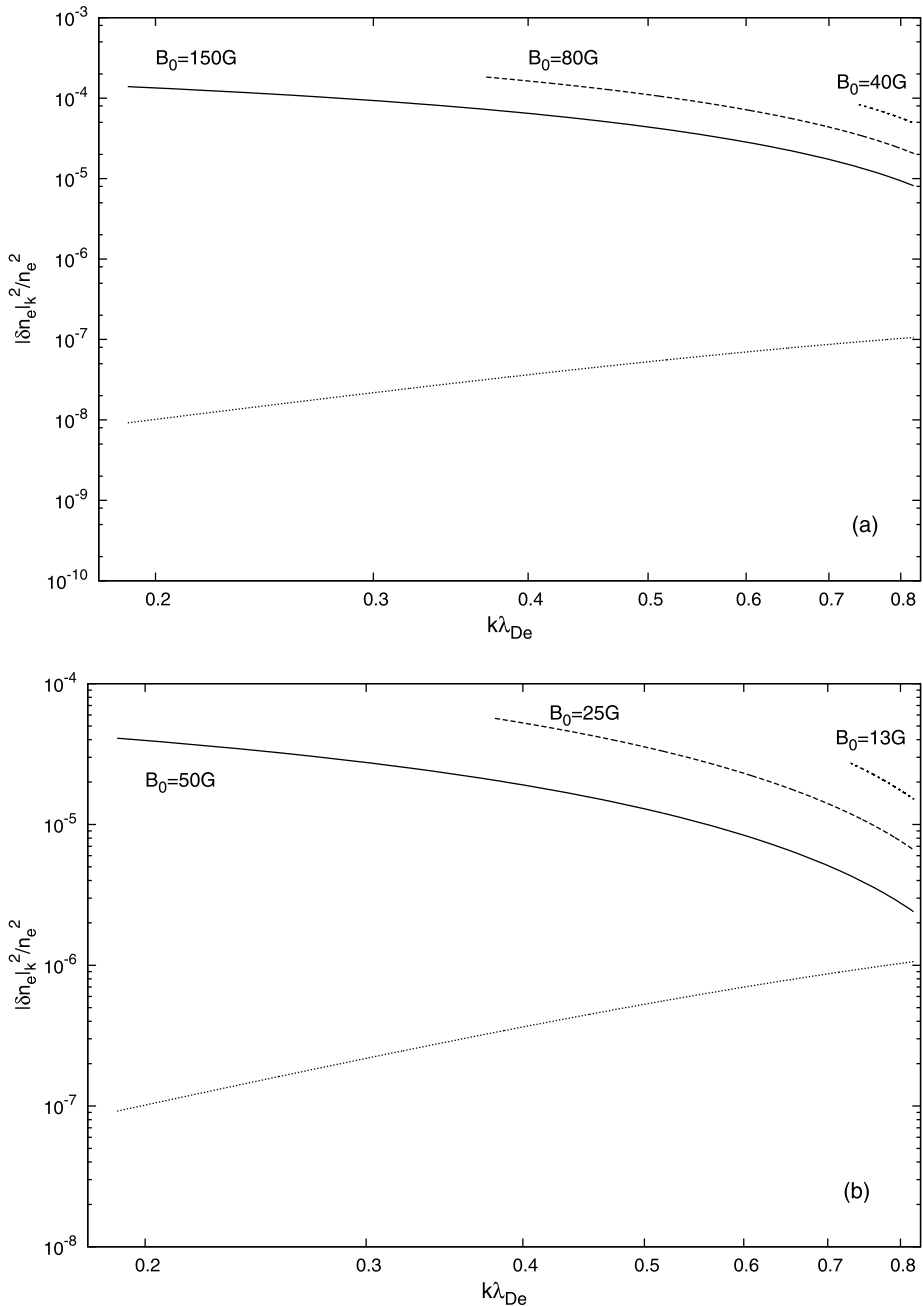


**Figure 5** Spectral density of electron density fluctuation versus  $k\lambda_{De}$  for the thermal level of ion-sound waves (dotted line), and when  $W_k^s/\omega_s = W_k^l/\omega_l$ . Here we used the following background plasma parameters  $n_0 = 2.8 \times 10^8 \text{ cm}^{-3}$ ;  $T_i/T_e = 0.5$ . Case (a) corresponds to  $T_e = 10^6$  K and three values of the magnetic field strength  $B_0 = 150$  G (solid line),  $B_0 = 80$  G (dashed line), and  $B_0 = 40$  G (dash-dotted line). Case (b) corresponds to  $T_e = 10^5$  K and three values of the magnetic field strength  $B_0 = 50$  G (solid line),  $B_0 = 25$  G (dashed line), and  $B_0 = 13$  G (dash-dotted line).

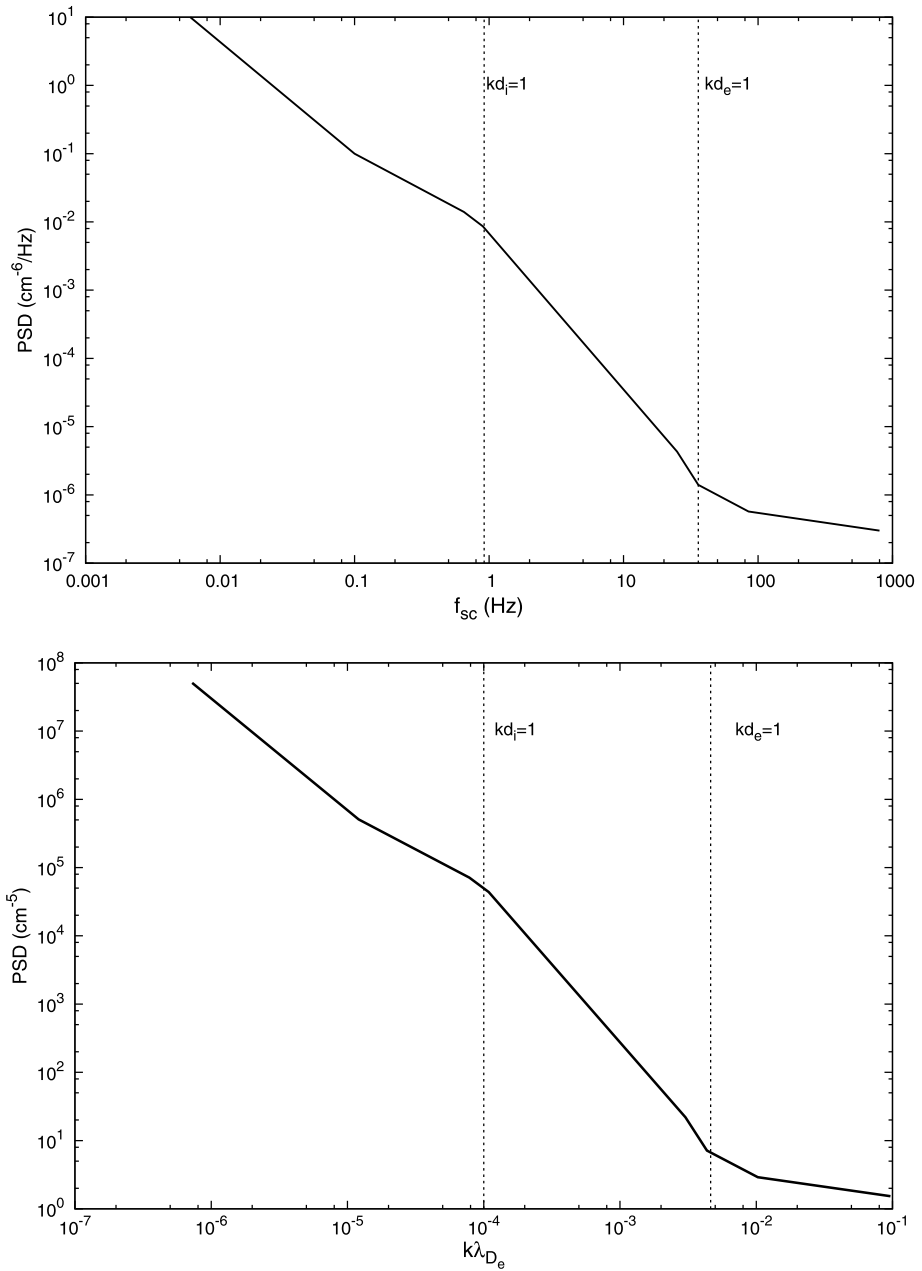


**Figure 6** Frequency-power spectra of Chen *et al.* (2012) of solar wind electron fluctuations (*top panel*), and *k*-power spectra of solar wind electron fluctuations (*bottom panel*). Here we used the following background solar wind plasma parameters:  $V_{SW} = 3.2 \times 10^7 \text{ cm s}^{-1}$ ,  $n_i = 16 \text{ cm}^{-3}$ , and  $T_e = 10^5 \text{ K}$  ( $\lambda_{De} = 616 \text{ cm}$ ).

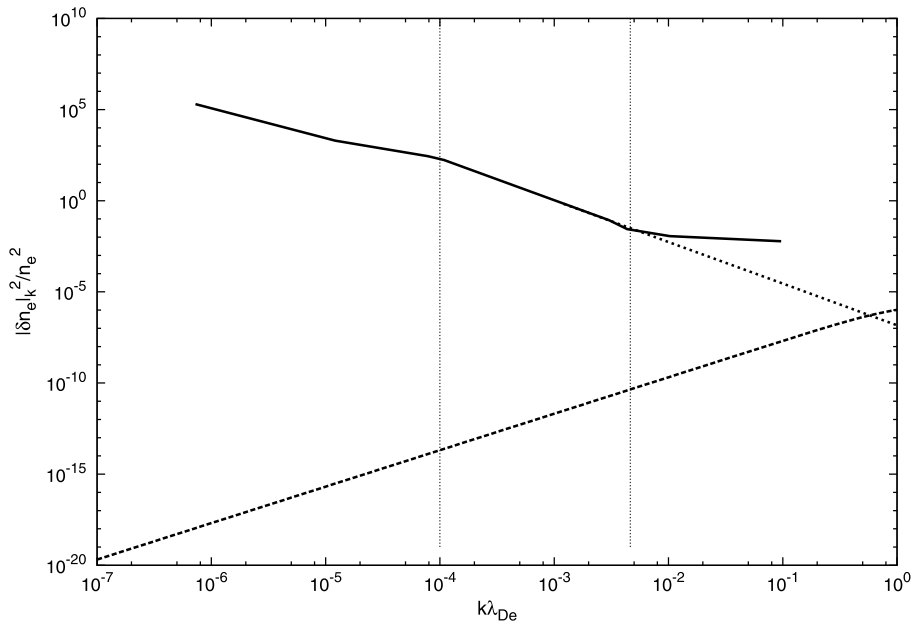


**Figure 7** Spectral density of electron density fluctuation versus  $k\lambda_{De}$  for the thermal level of ion-sound waves (*dashed line*), and the density fluctuation spectrum of solar wind turbulence given by Chen *et al.* (2012) (*solid line*). Here we used the following background plasma parameters:  $V_{SW} = 3.2 \times 10^7 \text{ cm s}^{-1}$ ,  $n_i = 16 \text{ cm}^{-3}$ , and  $T_e = 10^5 \text{ K}$  ( $\lambda_{De} = 616 \text{ cm}$ ) for the solar wind.

For emission at a frequency  $\omega_0$ , we then have

$$\tau = \frac{1}{3} \sqrt{\frac{2}{\pi}} \frac{e^2 \ln \Lambda}{m_e V_{Te}^3} \frac{1}{c\omega_0} \int_0^{1 \text{ AU}} \frac{\omega_{pe}^4(x)}{(\omega_0^2 - \omega_{pe}^2(x))^{1/2}} dx. \tag{25}$$

Assuming an exponential density profile  $n_e(x) = n_0 \exp(-x/H)$ , where  $x$  is the distance from the region of emission at density  $n_0$ , and  $H$  is the density scale height, we found the following expression (slightly corrected compared with Ratcliffe and Kontar, 2014) for the optical depth:

$$\tau = \frac{4}{9} \sqrt{\frac{2}{\pi}} \frac{e^2 \ln \Lambda}{m_e V_{Te}^3} \frac{H}{c} \left\{ \omega_0^2 - \frac{1}{\omega_0} [\omega_0^2 - \omega_{pe}^2(0)]^{1/2} [\omega_0^2 + 0.5\omega_{pe}^2(0)] \right\}. \tag{26}$$

As we consider a dense coronal plasma, we can use the reasonable value of  $H = 5 \times 10^9 \text{ cm}$  and find that

$$\tau \approx 2.8 \left[ \bar{\omega}_0^2 - \frac{1}{\bar{\omega}_0} (\bar{\omega}_0^2 - 1)^{1/2} (\bar{\omega}_0^2 + 0.5) \right], \tag{27}$$

where  $\bar{\omega}_0 = \omega_0/\omega_{pe}(0)$ .

As seen from Figure 8, the resulting escape fraction is rather high for  $f_{pe} = 0.2 \text{ GHz}$  for this density scale height. If for a different choice of parameters we could increase  $\tau$  by an order of magnitude, we would predict observable emissions due to quite high values of brightness temperature for the *f*- and *d*-processes.



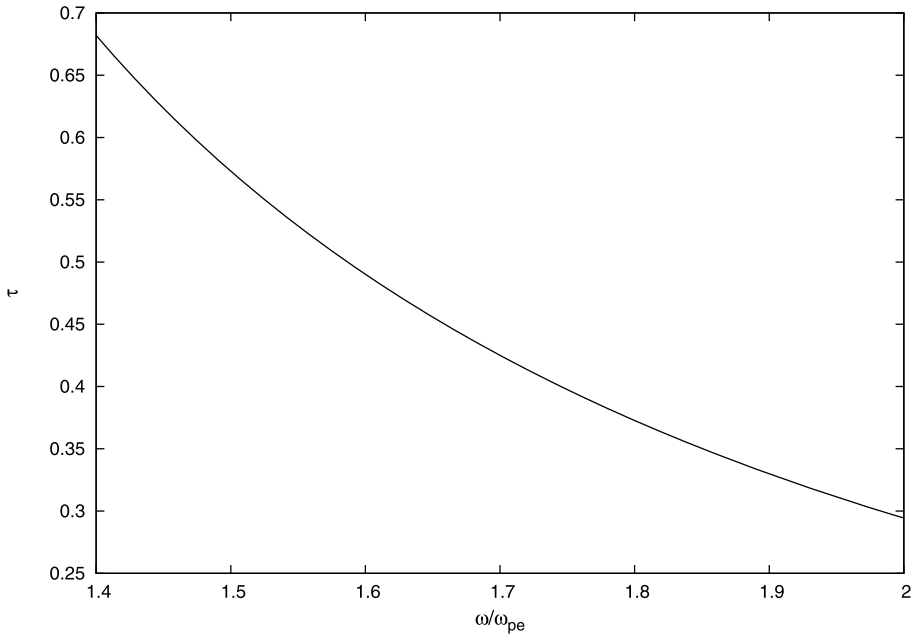


**Figure 8** Optical depth as a function of  $\omega/\omega_{pe}$  for  $H = 5 \times 10^9$  cm and  $f_{pe} = \omega_{pe}/2\pi = 0.2$  GHz.

#### 4. Application to Type I Solar Radio Bursts

Type I emission in noise storms is the most commonly observed radio phenomenon of the Sun (see review by Elgarøy, 1977; McLean and Labrum, 1985). Myriads of type I bursts, each lasting about a second, are superimposed on a continuum, which lasts from a few hours to days. Type I emission can extend from 50 to 500 MHz, peaking around 150–200 MHz. This activity occurs in active regions above sunspots with relatively strong magnetic fields. Type I emission is strongly ( $\approx 100\%$ ) circularly polarized, and there is only fundamental emission with no harmonic component. The brightness temperature is in the range from  $10^7$  to  $10^{10}$  K for continuum emissions and can exceed  $10^{11}$  K for bursts. The sizes of the emission sources are several arcminutes for the continuum and about 1 arcminute for bursts.

Currently, the plasma emission mechanism proposed by Melrose (1980a) is the most popular interpretation for type I radio emission. The plasma emission mechanism consists of two steps: i) an isotropic or loss-cone distribution of energetic electrons generates LWs, and ii) these LWs generate electromagnetic radiation (radio waves) via nonlinear coupling with ion-acoustic or other low-frequency waves. In these models, the type I continuum is explained by the LWs with effective temperature  $T_L \gtrsim 10^9$  K generated by a “gap electron distribution”. This implies a high level of low-frequency waves to ensure that the emission mechanism saturates at the radio brightness temperature  $T_T$  equal to the Langmuir wave temperature  $T_L$ . The increasing  $T_T$  during bursts is attributed to the local LW enhancements driven by the loss-cone instability. Theories based on the plasma emission mechanism have been developed in great detail (Benz and Wentzel, 1981; Spicer, Benz, and Huba, 1982; Wentzel, 1986; Thejappa, 1991).

One of the weak points of these theories is that the isotropic velocity distribution of electrons should give rise to the harmonic emission as well, which was never observed in

type I emission. In addition, a high level of low-frequency waves is required for the emission mechanism to saturate at a brightness temperature equal to the plasma wave temperature  $T_L$ .

We propose an alternative model for type I radio emission. The imbalanced turbulence of upward-propagating IAWs forms an asymmetric electron velocity distribution with a quasi-linear plateau in its forward half at  $\sqrt{1 + T_i/T_e} V_{Te} < V_{\parallel} < V_A$ . Landau damping of LWs propagating in the same direction in this velocity range is reduced, which enables the spontaneous growth of their amplitudes. In previous sections, we calculated the nonthermal level of these LWs and showed that it is sufficient to generate the observed type I radio emission. As the strongest radio emission is generated by LWs with phase velocities  $V_{LW} \lesssim V_A$ , the full plateau extending down to  $\sqrt{1 + T_i/T_e} V_{Te}$  is not required. In fact, it is sufficient that a narrower plateau is formed in the vicinity of  $V_{\parallel} \lesssim V_A$ .

Our estimations show that even with the thermal-level ion-acoustic waves, we obtain the observed brightness temperature for type I emission. The harmonic emission is never observed in type I storms; it does not occur in our model either, because the back-scattered LWs meet a strong Landau damping,  $\gamma_L \approx \omega_{pe}$ .

Our model works in low- $\beta$  plasmas, where the Alfvén velocity exceeds the electron thermal speed ( $V_A > V_{Te}$ ). Such conditions can be found in the solar corona at radial distances  $\approx 1.1$  solar radii, where type I storms are generated. Recent observations have demonstrated that magnetic fields above active regions at these distances can be strong enough, several 10s of G, and temperatures low, down to  $10^4$  K (see examples in Figure 8 by Schad *et al.*, 2016 with instances of  $B_0$  from 10 to 150 G, and the article by Antolin *et al.*, 2015 with coronal  $T_e$  from  $10^4$  to  $10^6$  K).

The often observed phenomenon of coronal rain provides a well-documented example of cold plasma patches created at high coronal levels by thermal instability (see Antolin *et al.*, 2015, and references therein). Plasma in the upper parts of long magnetic loops is especially prone to this instability. As the type I emission is generated, tentatively, at the tops of the highest magnetic loops overlapping active regions, the relatively cold plasma, produced there by thermal instability, may provide suitable conditions for type I radio emission.

We note that Dulk and McLean (1978) and Gopalswamy *et al.* (1986) proposed empirical models for the coronal  $B$  based on radio observations. In the model by Dulk and McLean (1978), the magnetic field strength depends on the plasma density model and assumes a particular generation mechanism for meter-wavelength radio bursts, with type I bursts excluded from the analysis. The model by Gopalswamy *et al.* (1986) is based on type I radio observations but assumes a particular generation mechanism for the bursts implying numerous shocks; it also critically depends on the radial profile of coronal density. It seems that the conditions above active regions are highly variable and can hardly be described in the framework of a single model. Therefore, instead of using a model, we refer to the values of the coronal magnetic field that are measured directly by Schad *et al.* (2016), which do not require assumptions of any specific plasma model or process. The measured values, several tens of gauss at relevant heliocentric distances  $R/R_{\odot} \approx 1.1$ , appeared to be higher than the values predicted in previous models. With these measured values of  $B$ , conditions for our scenario can be easily satisfied.

Additionally, we have to note that the current model reproduces the almost 100% polarization in the o-mode of type I bursts. The main reason is that the frequency of the emission due to the  $L \pm S \rightarrow T$  processes is below the cutoff frequency of the extraordinary (x-) mode,  $\omega_x = [\omega_{Be} + (\omega_{Be}^2 + 4\omega_{pe}^2)^{1/2}]/2$  for the values of the ratio,  $\omega_{Be}/\omega_{pe}$ , that are required in our model. The resulting electromagnetic emission then must be 100% in the o-mode.

## 5. Conclusions

We investigated the influence of imbalanced small-scale IAW turbulence on the spontaneous growth of LWs. The resulting high-amplitude LWs can generate type I radio emission that is observed above active regions in the solar corona.

Our starting point has been that the imbalanced turbulence of forward-propagating IAWs forms an asymmetric quasi-linear plateau in the forward half of the electron velocity distribution. This leads to the suppression of Landau damping for resonant LWs in the range of phase velocities  $\sqrt{1 + T_i/T_e} V_{Te} < V_{LW} < V_A$ . As a consequence, spontaneous excitation of high-amplitude LWs with  $W_L/W_{\text{therm}} \approx 10^7 - 10^9$  (for  $T_e = 10^6$  K) and  $W_L/W_{\text{therm}} \approx 10^5 - 10^7$  (for  $T_e = 10^5$  K) occurs in this velocity range. These LWs can produce strong electromagnetic radiation at the fundamental frequency close to the electron plasma frequency.

Even with the unfavorable thermal level of ion-sound waves, the brightness temperature of radio emission in our model is  $T_{T+} \approx 10^9 - 10^{11}$  K,  $T_{T-} \approx 10^{12} - 10^{15}$  K (for  $T_e = 10^6$  K) and  $T_{T+} \approx 10^8 - 10^{10}$  K,  $T_{T-} \approx 5 \times 10^9 - 10^{12}$  K (for  $T_e = 10^5$  K), which is high enough to explain observations. The bursts with extremely high brightness temperatures  $\gtrsim 10^{11}$  K can be more easily generated by the  $d$ -process. Moreover, our theory predicts 100% polarization in the o-mode of type I emission.

In conclusion, our model with the imbalanced IAW turbulence and spontaneously excited LWs provides a feasible explanation for solar type I radio emission. This model is also consistent with the fact that the first harmonic is never observed in type I radio emission.

Finally, we note that the 3D velocity distribution of electrons leads to a relativistic correction to the Landau damping of Langmuir waves (Melrose and Stenhouse, 1977) that may exceed the collisional damping assumed here. This effect applies to an isotropic electron distribution with a gap over some velocity range. The generalization of this gap model to the plateau model assumed here has yet to be investigated.

**Acknowledgements** The authors are thankful to the anonymous referee and to the Guest Editor Alexander Nindos for constructive comments. E.P.K. and N.H.B. were supported by Science and Technology Facilities Council Grant No. ST/L000741/1. Y.V. was supported by the Belgian Science Policy Office through IAP Programme, project P7/08 CHARM.

**Disclosure of Potential Conflicts of Interest** The authors declare that they have no conflicts of interest.

## Appendix A: The Parallel Electric Field of Dispersive Alfvén Waves

We follow Bian and Kontar (2011) and take the first moments of the linearized drift-kinetic equation for the electrons. This yields the linearized continuity equation

$$\frac{\partial n_e}{\partial t} + \nabla_{\parallel} n_0 u_{\parallel e} = 0, \quad (28)$$

where  $n_e/n_0$  is the electron density perturbation relative to a constant background  $n_0$ ,  $u_{\parallel e}$  is the parallel (to the magnetic field) component of the electron fluid velocity, and  $\nabla_{\parallel}$  denotes the spatial gradient along the magnetic field. The linearized parallel electron momentum equation is

$$n_0 m_e \frac{\partial u_{\parallel e}}{\partial t} = -T_e \nabla_{\parallel} n_e - n_0 e E_{\parallel}, \quad (29)$$

where we used  $p_e = n_e T_e$  for the pressure perturbation  $p_e$  and assumed a constant electron temperature  $T_e$ . The parallel component of the electric field  $E_{\parallel}$  is related to the electrostatic potential  $\phi$  and the parallel component of the magnetic vector potential  $A_{\parallel}$  via Faraday’s law,

$$E_{\parallel} = -\nabla_{\parallel}\phi - \frac{1}{c} \frac{\partial A_{\parallel}}{\partial t}. \tag{30}$$

The parallel component of Ampère’s law is

$$\nabla_{\perp}^2 A_{\parallel} = \frac{4\pi}{c} J_{\parallel}, \tag{31}$$

where  $\nabla_{\perp}$  is the spatial gradient perpendicular to the field, and it is assumed that the parallel current,

$$J_{\parallel} = -en_0 u_{e\parallel}, \tag{32}$$

is carried only by electrons. The system is closed by the quasi-neutrality condition

$$n_e = (\Gamma_0 - 1) \frac{en_0}{T_i} \phi, \tag{33}$$

where  $\Gamma_0$  is an integral operator that describes the average of the electrostatic potential over a ring of Larmor radius  $\rho_i$ . In Fourier space,  $\Gamma(b) = e^{-b} I_0(b)$  where  $b = \rho_i^2 k_{\perp}^2$  and  $I_0$  is the modified Bessel function. We use a simple Pade approximant for the operator  $\Gamma_0$  given by  $\Gamma_0(b) - 1 = -b/(1 + b)$ . Adopting the MHD normalization

$$(\hat{t}, \hat{\nabla}_{\parallel\perp}, \hat{A}_{\parallel}, \hat{\phi}, \hat{E}_{\parallel}) = \left( \frac{t}{\tau_A}, \nabla_{\parallel\perp} L, \frac{A_{\parallel}}{L B_0}, \frac{\phi c}{L V_A B_0}, \frac{E_{\parallel} c}{V_A B_0} \right) \tag{34}$$

with  $\tau_A = L/V_A$ , we therefore obtain

$$\partial_t n_e - \nabla_{\parallel} J_{\parallel} = 0, \tag{35}$$

$$\partial_t (\psi - d_e^2 J_{\parallel}) + \nabla_{\parallel} (\rho_s^2 n_e - \phi) = 0, \tag{36}$$

$$J_{\parallel} = \nabla_{\perp}^2 \psi, \tag{37}$$

$$(1 - \rho_i^2 \nabla_{\perp}^2) n_e = \nabla_{\perp}^2 \phi, \tag{38}$$

with  $\psi = -A_{\parallel}$ . This model generalizes the model that was previously discussed in Bian and Kontar (2010) to include the effect of electron inertia. The term proportional to  $d_e^2$  in Equation 36 can be rewritten as

$$E_{\parallel} = -\rho_s^2 \nabla_{\parallel} n_e + d_e^2 \partial_t J_{\parallel}. \tag{39}$$

This is Ohm’s law (the parallel electron momentum equation), and there are two contributions to the parallel electric field. The first is produced by electron density fluctuations along the magnetic field and involves the ion-sound Larmor radius  $\rho_s$  (the ion gyroradius at the electron temperature, *i.e.*  $\rho_s^2 = (T_e/T_i)\rho_i^2$ ). The second is produced by electron inertia and involves the electron skin depth  $d_e$ . The Alfvén wave equation is easily obtained from Equations 35–38 and reads

$$\partial_{tt} (\psi - d_e^2 \nabla_{\perp}^2 \psi) = \nabla_{\parallel}^2 [1 - (\rho_i^2 + \rho_s^2)] \nabla_{\perp}^2 \psi, \tag{40}$$

and hence the dispersion relation is

$$\omega = \pm k_{A\parallel} \sqrt{\frac{1 + k_{A\perp}^2 \rho_T^2}{1 + k_{A\perp}^2 d_e^2}}, \tag{41}$$

with  $\rho_T^2 = \rho_i^2 + \rho_s^2$ . We note that when  $\rho_T^2 = d_e^2$ , the dispersion relation is  $\omega = \pm k_{A\parallel}$ : the wave becomes non-dispersive and the wave-particle resonance reduces to a single point in velocity-space. Using the conductivity relation

$$\partial_t E_{\parallel} = (d_e^2 \partial_{tt} - \rho_s^2 \nabla_{\parallel}^2) J_{\parallel}, \tag{42}$$

we observe that the parallel electric field remains finite in the non-dispersive regime, *i.e.*  $|E_{\parallel}| = \rho_i^2 k_{A\parallel} k_{A\perp} |\delta B_{\perp}|$  in this case, its amplitude is proportional to the ion temperature. This property should be contrasted with the Hall-MHD (see Bian and Tsiklauri, 2009 and references therein), which is based on a cold ion assumption and therefore lacks a parallel electric field in the parameter regime  $\rho_s = d_e$ .

### Appendix B: An Angle-averaged Model for Fundamental Radio Emission

The kinetic Equation 9 for the processes  $L \pm S \rightarrow T$  may be written in the form

$$\begin{aligned} \frac{dW_{T\pm}(\mathbf{k}_T)}{dt} &= \pi \frac{\omega_{pe}^3}{4n_e T_e} \left(1 + \frac{3T_i}{T_e}\right) \int d\mathbf{k}_L d\mathbf{k}_S \\ &\times \omega_S \frac{[\mathbf{k}_T \times \mathbf{k}_L]^2}{k_T^2 k_L^2} \left[ \frac{W_L}{\omega_L} \left( \frac{W_S}{\omega_S} \mp \frac{W_T}{\omega_T} \right) - \frac{W_T}{\omega_T} \frac{W_S}{\omega_S} \right] \\ &\times \delta(\mathbf{k}_T - \mathbf{k}_L \mp \mathbf{k}_S) \delta(\omega_T - \omega_L \mp \omega_S), \end{aligned} \tag{43}$$

where  $W_L$ ,  $W_S$  and  $W_T$  are functions of their respective wavenumbers. First we perform the integral over  $\mathbf{k}_S$  using  $\delta(\mathbf{k}_T - \mathbf{k}_L \mp \mathbf{k}_S)$  to obtain

$$\begin{aligned} \frac{dW_{T\pm}(\mathbf{k}_T)}{dt} &= \pi \frac{\omega_{pe}^3}{4n_e T_e} \left(1 + \frac{3T_i}{T_e}\right) \int d\mathbf{k}_L \frac{[\mathbf{k}_T \times \mathbf{k}_L]^2}{k_T^2 k_L^2} \omega_S(\mathbf{k}_S) \\ &\times \left[ \frac{W_L(\mathbf{k}_L)}{\omega_L(\mathbf{k}_L)} \left( \frac{W_S(\mathbf{k}_S)}{\omega_S(\mathbf{k}_S)} \mp \frac{W_T(\mathbf{k}_T)}{\omega_T(\mathbf{k}_T)} \right) - \frac{W_T(\mathbf{k}_T)}{\omega_T(\mathbf{k}_T)} \frac{W_S(\mathbf{k}_S)}{\omega_S(\mathbf{k}_S)} \right] \\ &\times \delta(\omega_T(\mathbf{k}_T) - \omega_L(\mathbf{k}_L) \mp \omega_S(\mathbf{k}_S)). \end{aligned} \tag{44}$$

Here  $\mathbf{k}_S = \pm \mathbf{k}_T \mp \mathbf{k}_L$  for the  $f$ - and  $d$ -processes, respectively.

Assuming that the LWs and ion sound waves have some small angular spread in wavenumber space, covering a solid angle of  $\Delta\Omega$ , and further assuming that they are uniform within this spread, fundamental emission is produced approximately isotropically. So we define

$$W_{L,S}(\mathbf{k}) = \frac{1}{\Delta\Omega k^2} W_{L,S}^{Av}(k), \tag{45}$$

within  $\Delta\Omega$  the small solid angle occupied by the parent waves, and zero elsewhere, with  $W_{L,S}^{Av}(k)$  defined by

$$W_{L,S}^{Av}(k) = \iint k^2 \sin\theta W_{L,S}(\mathbf{k}) d\theta d\Phi, \tag{46}$$

and consider isotropic transverse waves

$$W_T(\mathbf{k}_T) = \frac{1}{4\pi k_T^2} W_T^{Av}(k_T), \tag{47}$$

$$W_T^{Av}(k) = \iint k^2 \sin\theta W_T(\mathbf{k}) d\theta d\Phi. \tag{48}$$

Writing  $d\mathbf{k}_L = k_L^2 \sin\theta dk_L d\theta d\Phi$  and substituting our definitions of the angle-averaged spectral energy density (expressions 45–46), we find for the first term in the square brackets

$$\begin{aligned} & \iint \sin^2\theta_{LT} \frac{W_L(\mathbf{k}_L) W_S(\mathbf{k}_S)}{\omega_L \omega_S} k_L^2 \sin\theta d\theta d\Phi \\ &= \frac{W_L^{Av}(k_L)}{\Delta\Omega\omega_L} \frac{W_S^{Av}(k_S)}{\Delta\Omega k_S^2 \omega_S} \iint \sin^2\theta_{LT} \sin\theta d\theta d\Phi \\ &= \frac{W_L^{Av}(k_L)}{\Delta\Omega\omega_L} \frac{W_S^{Av}(k_S)}{k_S^2 \omega_S} \langle \sin^2\theta_{LT} \rangle, \end{aligned} \tag{49}$$

where we assume that the average value of  $\sin^2\theta_{LT}$  is well defined and given by

$$\iint \sin^2\theta_{LT} \sin\theta d\theta d\Phi = \Delta\Omega \langle \sin^2\theta_{LT} \rangle. \tag{50}$$

Similarly, using expressions 45–48 for the second and third terms in square brackets, we write

$$\begin{aligned} & \iint \sin^2\theta_{LT} \frac{W_L(\mathbf{k}_L) W_T(\mathbf{k}_T)}{\omega_L \omega_T} k_L^2 \sin\theta d\theta d\Phi = \frac{W_L^{Av}(k_L)}{\omega_L} \frac{W_T^{Av}(k_T)}{4\pi k_T^2 \omega_T} \langle \sin^2\theta_{LT} \rangle \\ & \iint \sin^2\theta_{LT} \frac{W_T(\mathbf{k}_T) W_S(\mathbf{k}_S)}{\omega_T \omega_S} k_L^2 \sin\theta d\theta d\Phi = \frac{W_T^{Av}(k_T)}{4\pi k_T^2 \omega_T} \frac{W_S^{Av}(k_S)}{\omega_S} \langle \sin^2\theta_{LT} \rangle. \end{aligned} \tag{51}$$

Finally, the complete expression is

$$\begin{aligned} \frac{dW_{T\pm}^{Av}(k_T)}{dt} &= \pi \frac{\omega_{pe}^3}{4n_e T_e} \left( 1 + \frac{3T_i}{T_e} \right) \langle \sin^2\theta_{LT} \rangle \\ & \times \int dk_L \omega_S \delta(\omega_T - \omega_L \mp \omega_S) \\ & \times \left[ \frac{W_L^{Av}(k_L)}{\omega_L} \frac{4\pi k_T^2}{\Delta\Omega k_S^2} \frac{W_S^{Av}(k_S)}{\omega_S} \mp \frac{W_L^{Av}(k_L)}{\omega_L} \frac{W_T^{Av}(k_T)}{\omega_T} - \frac{W_T^{Av}(k_T)}{\omega_T} \frac{W_S^{Av}(k_S)}{\omega_S} \right], \end{aligned} \tag{52}$$

where  $k_S^2 = k_T^2 + k_L^2$ .

Now, using  $\delta(\omega_T - \omega_L \mp \omega_S)$  to integrate over  $k_L$ , for  $k_T^2 d_e^2 \gg \frac{1}{3} \frac{m_e}{m_i}$ , we obtain

$$\begin{aligned} \frac{dW_{T\pm}^{Av}(k_T)}{dt} &= \frac{\pi \omega_{pe}^4 V_s}{24 n_e T_e V_{Te}^2} \left( 1 + \frac{3T_i}{T_e} \right) \\ &\times \left[ \frac{W_L^{Av}(k_L)}{\omega_L} \frac{4\pi k_T^2}{\Delta\Omega k_S^2} \frac{W_S^{Av}(k_S)}{\omega_S} \mp \frac{W_L^{Av}(k_L)}{\omega_L} \frac{W_T^{Av}(k_T)}{\omega_T} - \frac{W_T^{Av}(k_T)}{\omega_T} \frac{W_S^{Av}(k_S)}{\omega_S} \right]. \end{aligned} \tag{53}$$

Here  $k_L \approx \mp \frac{k_T d_e}{\sqrt{3} \lambda_{De}}$ , and we have evaluated the average  $\langle \sin^2 \theta_{LT} \rangle$  over a sphere, which gives a value of 1/2.

### Appendix C: Spectral Density of the Electron Density Fluctuation due to Ion-Sound Waves

The relationship between the electric field and density perturbations that are due to ion-sound waves is

$$\delta \mathbf{E} = -\frac{T_e}{n_e e} \nabla \delta n. \tag{54}$$

We can rewrite the above expression as

$$\frac{|\mathbf{E}_k|^2}{4\pi} = \frac{1}{4\pi} \left( \frac{T_e}{n_e e} \right)^2 k_s^2 |\delta n_c|_k^2. \tag{55}$$

According to Tsytovich and ter Haar (1995), the occupation number  $N_k$  is related to  $\mathbf{E}_k$  as

$$N_k^l = \frac{\pi^2}{\hbar} \left( \frac{1}{\omega^2} \frac{\partial}{\partial \omega} \omega^2 \varepsilon^l \right) \Big|_{\omega=\Omega^l(k)} |\mathbf{E}_k^l|^2, \tag{56}$$

where the index  $l$  denotes longitudinal waves. We can rewrite this expression using  $\varepsilon^l(\Omega^l, \mathbf{k}) = 0$  and

$$N_k^l = \frac{(2\pi)^3 W_k^l}{\hbar \Omega^l(\mathbf{k})}, \tag{57}$$

as

$$W_k^l = \frac{1}{8\pi} \omega \frac{\partial \varepsilon^l}{\partial \omega} \Big|_{\omega=\Omega^l(k)} |\mathbf{E}_k^l|^2. \tag{58}$$

For ion-sound waves

$$\varepsilon^s \approx 1 - \frac{\omega_{pi}^2}{\omega_s^2} + \frac{1}{(k_s \lambda_{De})^2}, \tag{59}$$

which gives the following dispersion relations for ion-sound waves:

$$\omega_s \simeq \frac{k_s V_s}{\sqrt{1 + k_s^2 \lambda_{De}^2}}. \tag{60}$$

According to expression 59,

$$\frac{\partial \varepsilon^s}{\partial \omega_s} = 2 \frac{\omega_{\text{pi}}^2}{\omega_s^3}. \quad (61)$$

Combining Equations 61 and 58 gives

$$W_k^s = \frac{\omega_{\text{pi}}^2}{\omega_s^2} \frac{|E_k^s|^2}{4\pi}, \quad (62)$$

or using the dispersion relation 60, we can rewrite it as

$$W_k^s = \frac{(1 + k_s^2 \lambda_{\text{De}}^2)}{k_s^2 \lambda_{\text{De}}^2} \frac{|E_k^s|^2}{4\pi}. \quad (63)$$

Inserting this expression into Equation 55 and noting that  $\lambda_{\text{De}}^2 = T_e / (4\pi n_e e^2)$ , we obtain that the spectral energy density of ISWs is related to the spectral density of the electron density fluctuation as

$$\frac{W_k^s}{n_e T_e} = (1 + k_s^2 \lambda_{\text{De}}^2) \frac{|\delta n_e|_k^2}{n_e^2}. \quad (64)$$

Here the following normalization is used:

$$\int (\delta n_e^s)_k^2 dk = (\delta n_e)^2, \quad (65)$$

$$\int W_k^s dk = W^s. \quad (66)$$

Using that

$$(\delta n_e)_k^2 = \frac{(\delta n_e)_k^2}{4\pi k_s^2}, \quad (67)$$

and

$$W_k^s = \frac{W_k^s}{4\pi k_s^2}, \quad (68)$$

we can rewrite Equation 64 for the one-dimensional case as

$$\frac{W_k^s}{n_e T_e} = (1 + k_s^2 \lambda_{\text{De}}^2) \frac{|\delta n_e|_k^2}{n_e^2}. \quad (69)$$

## References

- Antolin, P., Vissers, G., Pereira, T.M.D., Roupe van der Voort, L., Scullion, E.: 2015, The multithermal and multi-stranded nature of coronal rain. *Astrophys. J.* **806**, 81. [DOI](#). [ADS](#).
- Artemyev, A.V., Zimovets, I.V., Rankin, R.: 2016, Electron trapping and acceleration by kinetic Alfvén waves in solar flares. *Astron. Astrophys.* **589**, A101. [DOI](#). [ADS](#).
- Banerjee, D., Teriaca, L., Doyle, J.G., Wilhelm, K.: 1998, Broadening of SI VIII lines observed in the solar polar coronal holes. *Astron. Astrophys.* **339**, 208. [ADS](#).
- Benz, A.O., Wentzel, D.G.: 1981, Coronal evolution and solar type I radio bursts – an ion-acoustic wave model. *Astron. Astrophys.* **94**, 100. [ADS](#).



- Bian, N.H., Kontar, E.P.: 2010, A gyrofluid description of Alfvénic turbulence and its parallel electric field. *Phys. Plasmas* **17**(6), 062308. [DOI](#). [ADS](#).
- Bian, N.H., Kontar, E.P.: 2011, Parallel electric field amplification by phase mixing of Alfvén waves. *Astron. Astrophys.* **527**, A130. [DOI](#). [ADS](#).
- Bian, N.H., Tsiklauri, D.: 2009, Compressible Hall magnetohydrodynamics in a strong magnetic field. *Phys. Plasmas* **16**(6), 064503. [DOI](#). [ADS](#).
- Bian, N.H., Kontar, E.P., Brown, J.C.: 2010, Parallel electric field generation by Alfvén wave turbulence. *Astron. Astrophys.* **519**, A114. [DOI](#). [ADS](#).
- Bruno, R., Carbone, V.: 2013, The solar wind as a turbulence laboratory. *Living Rev. Solar Phys.* **10**, 2. [DOI](#). [ADS](#).
- Chaston, C.C., Salem, C., Bonnell, J.W., Carlson, C.W., Ergun, R.E., Strangeway, R.J., McFadden, J.P.: 2008, The Turbulent Alfvénic Aurora. *Phys. Rev. Lett.* **100**(17), 175003. [DOI](#). [ADS](#).
- Chen, C.H.K., Salem, C.S., Bonnell, J.W., Mozer, F.S., Bale, S.D.: 2012, Density fluctuation spectrum of solar wind turbulence between ion and electron scales. *Phys. Rev. Lett.* **109**(3), 035001. [DOI](#). [ADS](#).
- Dulk, G.A., McLean, D.J.: 1978, Coronal magnetic fields. *Solar Phys.* **57**, 279. [DOI](#). [ADS](#).
- Elgarøy, E.Ø.: 1977, *Solar Noise Storms*, Pergamon Press, Oxford. [ADS](#).
- Goertz, C.K., Boswell, R.W.: 1979, Magnetosphere-ionosphere coupling. *J. Geophys. Res.* **84**, 7239. [DOI](#). [ADS](#).
- Gopalswamy, N., Thejappa, G., Sastry, C.V., Tlamicha, A.: 1986, Estimation of coronal magnetic fields using Type-I emission. *Bull. Astron. Inst. Czechoslov.* **37**, 115. [ADS](#).
- Hamilton, R.J., Petrosian, V.: 1987, Generation of plasma waves by thick-target electron beams, and the expected radiation signature. *Astrophys. J.* **321**, 721. [DOI](#). [ADS](#).
- Hasegawa, A., Chen, L.: 1975, Kinetic process of plasma heating due to Alfvén wave excitation. *Phys. Rev. Lett.* **35**, 370. [DOI](#). [ADS](#).
- He, J., Tu, C., Marsch, E., Yao, S.: 2012, Do oblique Alfvén/Ion-cyclotron or fast-mode/Whistler waves dominate the dissipation of solar wind turbulence near the proton inertial length? *Astrophys. J. Lett.* **745**, L8. [DOI](#). [ADS](#).
- Kontar, E.P., Ratcliffe, H., Bian, N.H.: 2012, Wave-particle interactions in non-uniform plasma and the interpretation of hard X-ray spectra in solar flares. *Astron. Astrophys.* **539**, A43. [DOI](#). [ADS](#).
- Lysak, R.L., Lotko, W.: 1996, On the kinetic dispersion relation for shear Alfvén waves. *J. Geophys. Res.* **101**, 5085. [DOI](#). [ADS](#).
- Marsch, E., Tu, C.-Y.: 1990, Spectral and spatial evolution of compressible turbulence in the inner solar wind. *J. Geophys. Res.* **95**, 11945. [DOI](#). [ADS](#).
- Matthaeus, W.H., Zank, G.P., Oughton, S., Mullan, D.J., Dmitruk, P.: 1999, Coronal heating by magnetohydrodynamic turbulence driven by reflected low-frequency waves. *Astrophys. J. Lett.* **523**, L93. [DOI](#). [ADS](#).
- McLean, D.J., Labrum, N.R.: 1985, *Solar Radiophysics: Studies of Emission from the Sun at Metre Wavelengths*, Cambridge University Press, Cambridge. [ADS](#).
- Melrose, D.B.: 1980a, A plasma-emission mechanism for type I solar radio emission. *Solar Phys.* **67**, 357. [DOI](#). [ADS](#).
- Melrose, D.B.: 1980b, *Plasma Astrophysics: Nonthermal Processes in Diffuse Magnetized Plasmas. Astrophysical Applications 2*, Gordon and Breach Science Publishers, New York. [ADS](#).
- Melrose, D.B., Stenhouse, J.E.: 1977, Emission and absorption of Langmuir waves by anisotropic unmagnetized particles. *Aust. J. Phys.* **30**, 481. [ADS](#).
- Melrose, D.B., Wheatland, M.S.: 2014, Bulk energization of electrons in solar flares by Alfvén waves. *Solar Phys.* **289**, 881. [DOI](#). [ADS](#).
- Morton, R.J., Tomczyk, S., Pinto, R.: 2015, Investigating Alfvénic wave propagation in coronal open-field regions. *Nat. Commun.* **6**, 7813. [DOI](#). [ADS](#).
- Pierrard, V., Voitenko, Y.: 2013, Modification of proton velocity distributions by Alfvénic turbulence in the solar wind. *Solar Phys.* **288**, 355. [DOI](#). [ADS](#).
- Ratcliffe, H.: 2013, Electron beam evolution and radio emission in the inhomogeneous solar corona. PhD thesis, University of Glasgow, United Kingdom. [ADS](#).
- Ratcliffe, H., Kontar, E.P.: 2014, Plasma radio emission from inhomogeneous collisional plasma of a flaring loop. *Astron. Astrophys.* **562**, A57. [DOI](#). [ADS](#).
- Reid, H.A.S., Kontar, E.P.: 2010, Solar wind density turbulence and solar flare electron transport from the Sun to the Earth. *Astrophys. J.* **721**, 864. [DOI](#). [ADS](#).
- Rudakov, L., Crabtree, C., Ganguli, G., Mithaiwala, M.: 2012, Quasilinear evolution of plasma distribution functions and consequences on wave spectrum and perpendicular ion heating in the turbulent solar wind. *Phys. Plasmas* **19**(4), 042704. [DOI](#). [ADS](#).
- Ryutov, D.D.: 1969, Quasilinear relaxation of an electron beam in an inhomogeneous plasma. *Sov. Phys. JETP* **30**, 131. [ADS](#).

- Schad, T.A., Penn, M.J., Lin, H., Judge, P.G.: 2016, Vector magnetic field measurements along a cooled stereo-imaged coronal loop. *Astrophys. J.* **833**, 5. DOI. ADS.
- Spicer, D.S., Benz, A.O., Huba, J.D.: 1982, Solar type I noise storms and newly emerging magnetic flux. *Astron. Astrophys.* **105**, 221. ADS.
- Stasiewicz, K., Bellan, P., Chaston, C., Kletzing, C., Lysak, R., Maggs, J., Pokhotelov, O., Seyler, C., Shukla, P., Stenflo, L., Streltsov, A., Wahlund, J.-E.: 2000, Small scale Alfvénic structure in the aurora. *Space Sci. Rev.* **92**, 423. ADS.
- Thejappa, G.: 1991, A self-consistent model for the storm radio emission from the Sun. *Solar Phys.* **132**, 173. DOI. ADS.
- Tsytovich, V.N., ter Haar, D.: 1995, *Lectures on Non-linear Plasma Kinetics*, Springer, Berlin. ADS.
- Vedenov, A.A., Velikhov, E.P.: 1963, Quasilinear approximation in the kinetic theory of a low-density plasma. *Sov. Phys. JETP* **16**, 682. ADS.
- Voitenko, Y., De Keyser, J.: 2016, MHD-kinetic transition in imbalanced Alfvénic turbulence. *Astrophys. J. Lett.* **832**, L20. DOI. ADS.
- Voitenko, Y., Goossens, M.: 2000, Nonlinear decay of phase-mixed Alfvén waves in the solar corona. *Astron. Astrophys.* **357**, 1073. ADS.
- Voitenko, Y., Goossens, M.: 2006, Energization of plasma species by intermittent kinetic Alfvén waves. *Space Sci. Rev.* **122**, 255. DOI. ADS.
- Voitenko, Y., Pierrard, V.: 2013, Velocity-space proton diffusion in the solar wind turbulence. *Solar Phys.* **288**, 369. DOI. ADS.
- Voitenko, Y.M.: 1998, Excitation of kinetic Alfvén waves in a flaring loop. *Solar Phys.* **182**, 411. DOI. ADS.
- Warmuth, A., Mann, G.: 2005, A model of the Alfvén speed in the solar corona. *Astron. Astrophys.* **435**, 1123. DOI. ADS.
- Wentzel, D.G.: 1986, A theory for the solar type-I radio continuum. *Solar Phys.* **103**, 141. DOI. ADS.